CHAPTER 2

Development of experimental setups for robot assisted incremental sheet forming (RAISF) and robot assisted incremental sheet hydroforming (RAISHF)

2.1 Introduction

An experimental setup for RAISF and RAISHF has been developed from scratch at mechanical engineering department at IITBHU. This work is an extension of the earlier work carried out by Santosh Kumar and Yogesh Kumar [123, 132, 133], in which CNC-based incremental sheet hydroforming setup was fabricated. Experiments on aluminium, copper and titanium-based sheets were conducted by producing conical, pyramidal and multi-feature geometry. In the current work, six-axis industrial robotic arm has been used for performing ISHF. A robotic arm has various advantages over CNC machine as given below:

(a) Increased forming can pace up the process and decrease the forming time

(b) Increased reach and workspace can enhance the capability of the process so that it can deform larger sheets which are used in automobile and aerospace sectors [134].

(c) Robotic arms provide better control of the process causing parts to be formed with better accuracy and precision.

(d) Robots have higher degrees of freedom as compared to CNC machines, due to which multi-dimensional translatory and rotatory motion can be achieved for getting more complex and intricate geometries.

2.1.1 The Experimental Apparatus

The experimental setup for RAISF and RAISHF consists of the following main parts.

2.1.2 Six Axis Industrial Robotic Arm

The robotic arm as supplied by Yaskawa robot Pvt. Ltd has been established on robust Table fabricated at Production lab of the IIT BHU, having six motors providing translatory and rotatory motion to the manipulator. The payload for the robotic arm is 180 kN. The robotic arm is equipped with a teach pendant on which the tool path programme is fed. The controller contains all the electronic circuits of the robotic arm. The details of the robotic arm is given in Figure 2.1(a) - (e).

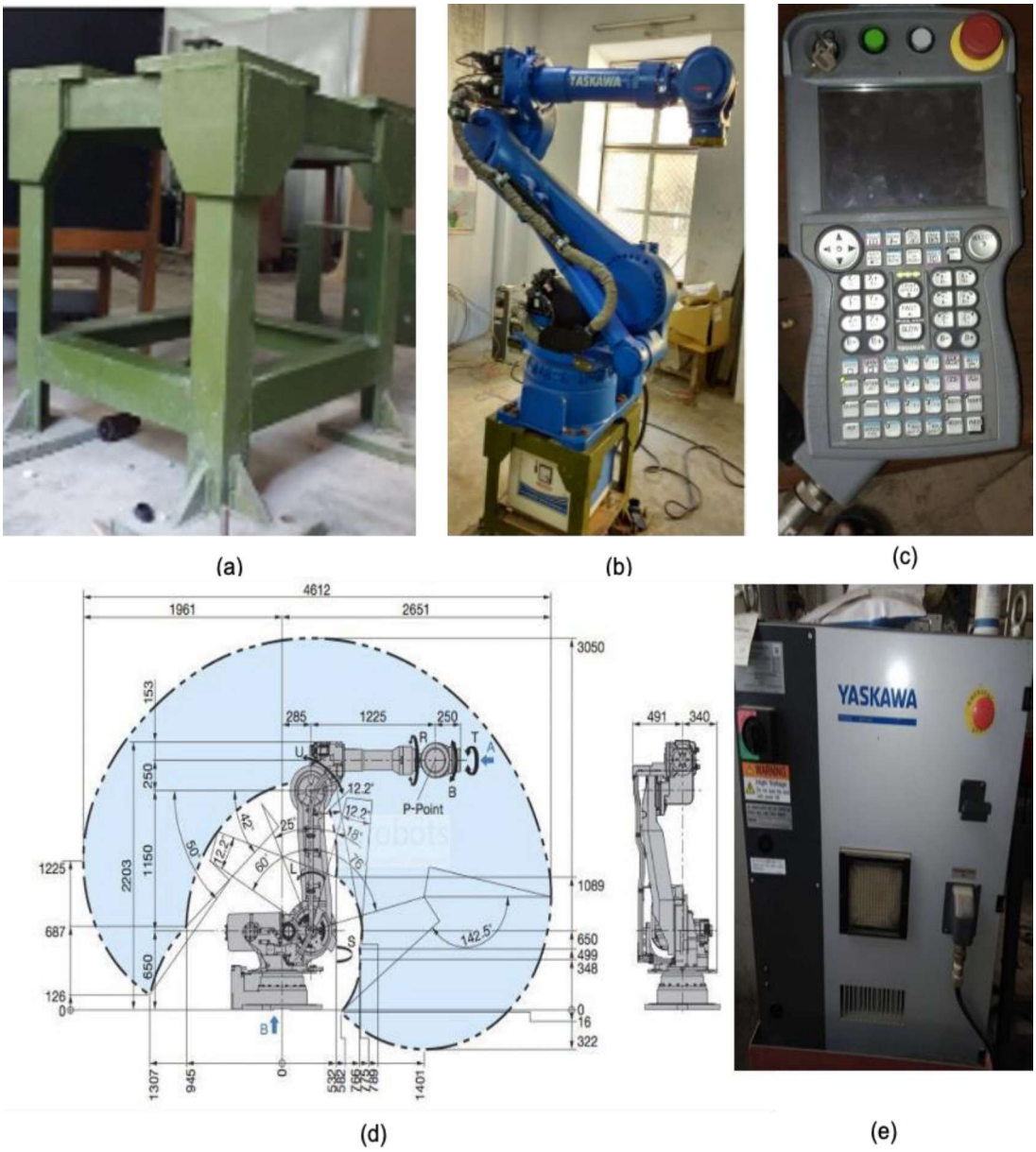

Figure 2.1: Details of the robotic arm: (a) Stand for robotic arm installation, (b) Installed robotic arm (YASKAWA), (c) Teach pendant for online programming, (d) Measurements associated with the robotic arm, and (e)DX-200 Controller for robotic arm.

2.1.3 Forming tool

The forming tool plays the most crucial role in the ISF. For this work, two types of forming tools of HSS have been fabricated. (a) Roller ball tool (b) Fixed ball tool of diameter 10,

12.5 and 15 mm. Various forming tools are shown in Figure 2.2 (a). The primary distinction between these two roller types lies in their contact friction characteristics. In the rolling ball tool, there is a rolling motion between the rollers and the sheet, resulting in static friction. Conversely, in the case of the fixed ball tool, it slides along the surface of the sheet, resulting in kinetic friction between the tool and the sheet.

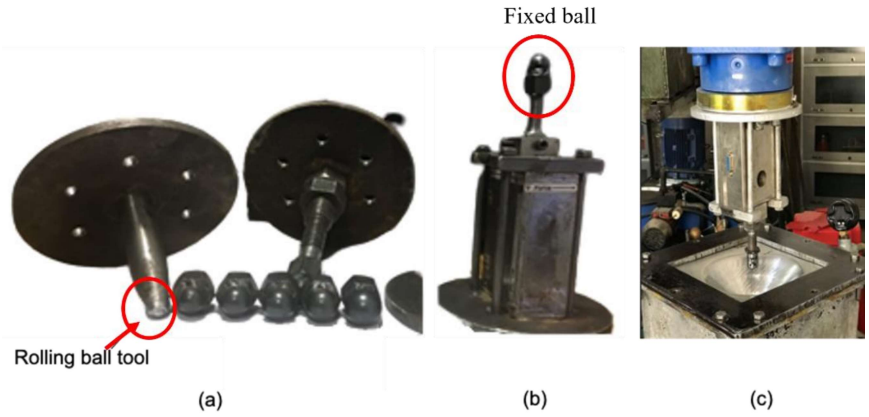

Figure 2.2: (a) Various forming tools, (b) Forming tool with tool dynamometer, and (c) Complete forming tool mounted on robotic arm.

From the initial experimentations using straight groove test it has been revealed that fixed ball tool shown in Figure 2.2(b) gives better formability than roller ball tool. The reason can be the underlying friction condition which is kinetic (limiting) in nature. Limiting friction has larger magnitude than that of static friction. More frictional dissipation can give rise to more localized softening of sheet in direct contact with the sheet and hence formability can be enhanced.

2.1.4 Fluid chamber and Hydraulic circuit

For accomplishment of RAISHF process, fluid (HP ENKLO 68 hydraulic oil) is fed from back side of the sheet. The fluid is kept in a fluid chamber which applies hydrostatic pressure to the side of the sheet which is in contact with the sheet. This hydrostatic pressure plays a key role in improvement of surface finish, dimensional accuracy and reduction of

spring back from the final product. The experimental setup with hydraulic circuit is shown in Figure 2.3.

Once the sheet is clamped and programming is done on the robotic arm, pressurized fluid is fed from back side of the fluid using hydraulic circuit. Initially valve 2 and valve 3 are open and valve 1 is closed. Once the fluid chamber is filled with fluid by manual feeding, valve 2 is closed. A counter weight is put on the piston for maintaining pressure in the chamber. The piston moves up and down to maintain the pressure within the chamber which was measured by a pressure gauge attached on the fluid chamber. Once the forming is complete, valve 2 and valve 1 are opened and fluid is released back to the fluid chamber.

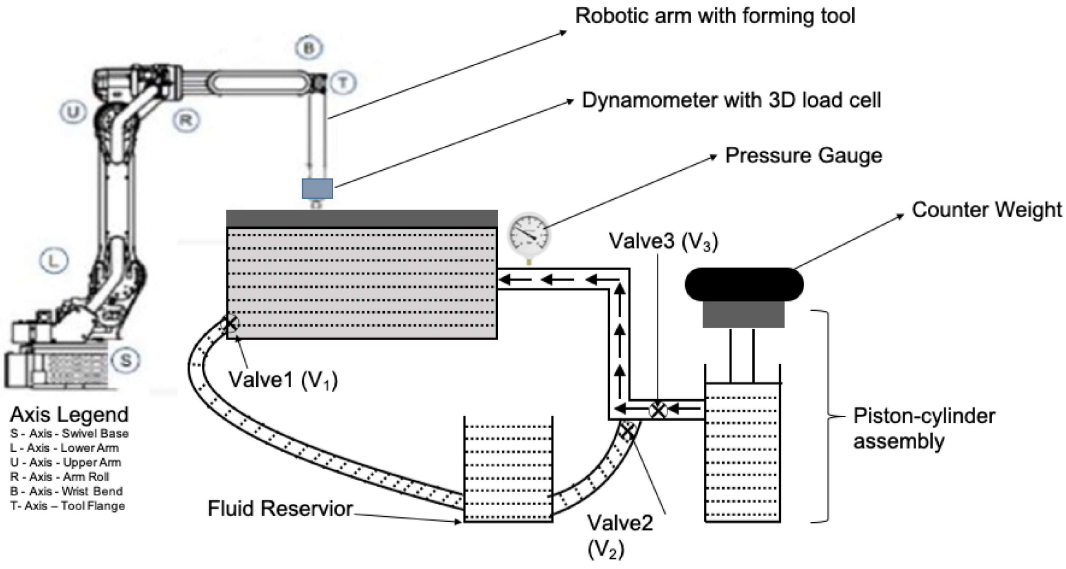

Figure 2.3: RAISHF with hydraulic circuit

The complete setup with robotic arm, mounted forming tool with dynamometer and hydraulic chamber is shown in Figure 2.4.

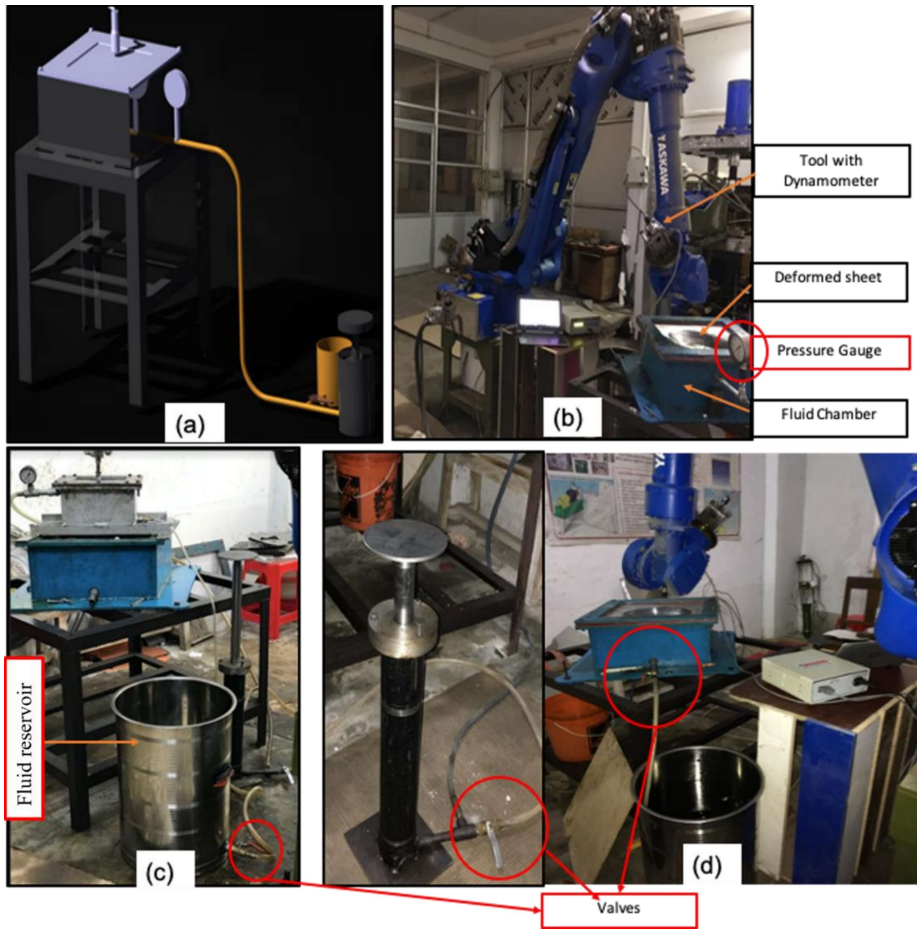

Figure 2.4: Complete fixture of RAISF and RAISHF (a) CAD model of RASIHF (b) established setup at IITBHU, (c) fluid reservoir, and (d) piston assembly with valves and fluid filled chamber

2.2 Tool path programming

For tool path programming, two types of methods can be adopted.

(1) Teach pendant based tool path programming

(2) Software based tool path programming:

2.2.1 Teach pendant based tool path programming

This is also called online method of tool path programming. In this method, the conical shape of the fixed wall angle is first generated on CATIA V5R20 software. Once the shape generated has been on CATIA V5R20, the online tool path planning is done for robotic ISF

using the Teach pendant. The tool path planning for axis-symmetric and non-axis symmetric shapes with fixed wall angles has been done successfully, the strategy of which is elaborated by a sample program for generating an axis-symmetric cone, as shown in Figure 2.5.

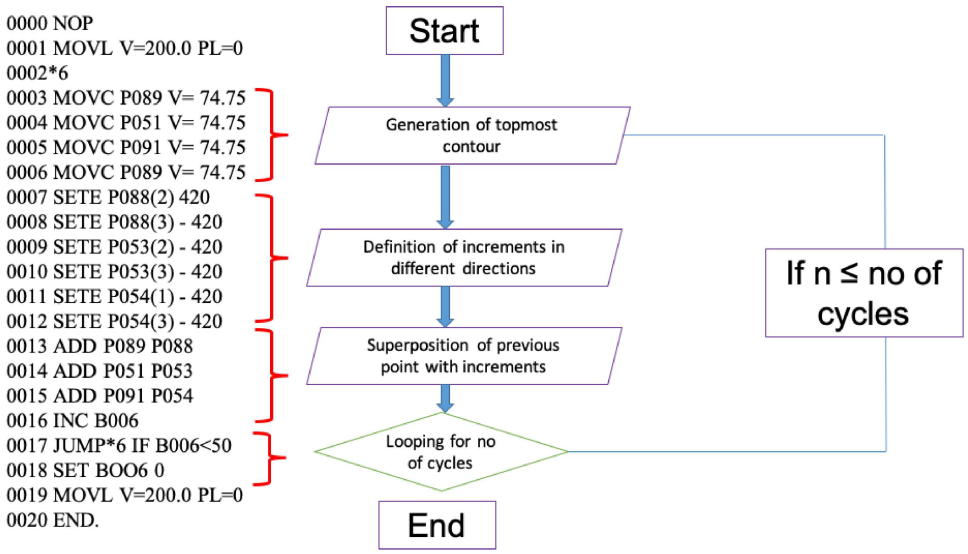

Figure 2.5: Strategy for generating tool path: A sample program for axis symmetric cone.

2.2.2 Software based tool path planning

This is also called offline method of tool path planning and programming. In this method, shapes and tool paths, after successfully generated on CATIAV5R20, are fed directly into the RobotDK software. The flow diagram of the process of tool path generation in the offline mode of tool path planning is shown in Figure 2.6.

Teach pendant-based tool path planning method is fast, but its application is restricted to forming a limited number of shapes. However, any general shape can be made using software-based programming methods. So, depending on the application, the user can select the strategy for fabrication.

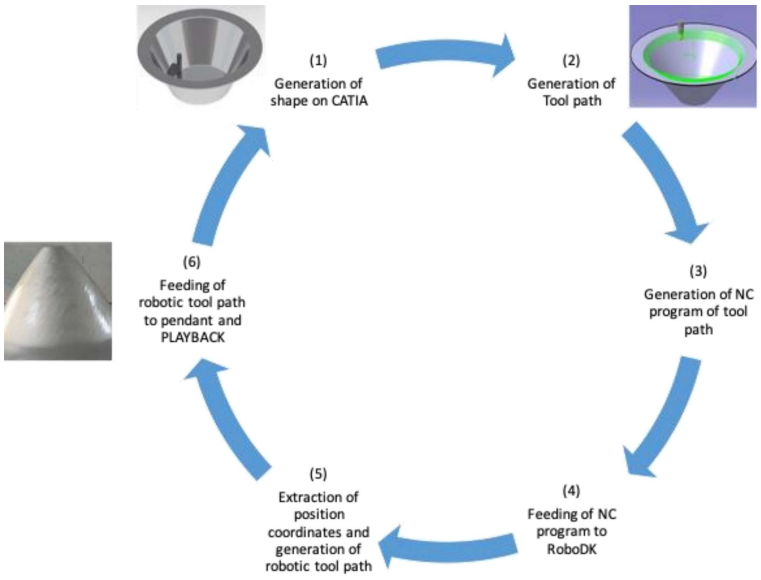

Figure 2.6: Software based tool path programming strategy.

2.3 Materials for experimentation

Aluminium and its alloys are highly versatile materials with a wide range of applications. Aluminium is a lightweight metal known for its excellent strength-to-weight ratio, corrosion resistance, and has good electrical conductivity. These properties make it a popular choice in various industries. One of the key advantages of aluminium and its alloys is their low density, which makes them ideal for applications where weight reduction is essential. Industries such as aerospace, automotive, and transportation benefit greatly from aluminium's lightweight nature, as it helps in improving fuel efficiency and overall performance. These alloys also exhibit excellent formability and allow for intricate shaping and complex designs as can be easily extruded, cast, or rolled into various shapes and sizes, offering manufacturers a high degree of flexibility. This versatility has made aluminium alloys a preferred choice in industries such as construction, consumer electronics, and packaging. Aluminium alloys offer even greater benefits by combining aluminium with other elements to enhance specific properties. For example, the addition of copper, magnesium, or zinc significantly increases the strength and hardness of the alloy, making

it suitable for structural components. Additionally, alloying elements like silicon and manganese improves corrosion resistance of aluminium alloys.

2.3.1 Aluminium lloy designation system

As per the Aluminum Association, the wrought aluminium alloy is normally designated by 4-digit system XXXX, where the first digit indicates the alloy group, or major alloy addition. The second digit represents modification of original alloy or impurity limits and the last two digits identify the specific aluminium alloy. Experimental alloys also use this system, but are indicated as experimental by the prefix X. The designation system for wrought aluminium alloys and cast alloys are presented in Table 2.1.

Table 2.1: Four-digit Aluminium alloy designation system for wrought alloys

Four-digit series	Al content or main alloying elements
1XXX	99.00% minimum
2XXX	Copper
3XXX	Manganese
4XXX	Silicon
5XXX	Magnesium
6XXX	Magnesium and Silicon
7XXX	Zinc (most also contain Mg)
8XXX	Others eg. Lithium
9XXX	Unused

In the current work, aluminium alloy AA6061 has been used. Aluminium is being widely used in the automobile and aerospace industries owing to following properties.

(a) High strength to weight ratio can lead to light weightiness of the vehicle.

(b) Good corrosion resistive properties.

(c) Almost 90% of used Aluminum is recyclable at the end of the process which can lead to better environmental consequences.

(d) Good combination of strength and ductility.

2.4 Design of experiments

The main parameters affecting forming force, formability and surface finish of the product formed by ISF, are tool speed, tool diameter and step depth. For design of experiments, standard straight groove tests have been conducted on nine samples, in different forming conditions. The surface of each sample has been engraved with circular grid patterns of 5mm diameter for strain analysis. For engraving, a 50 W Fibre Laser has been used, as shown in Fig. 2.7 (a). Three parameters have been chosen as input variables. These are tool diameters of 10 mm, 12.5mm, and 15 mm, vertical step depths of 0.2mm, 0.4mm, and 0.6 mm, and tool speed of 50 mm/s, 100 mm/s, and 150 mm/s. Different values of the input parameters accounted for different levels in regression analysis. Different values assigned as various levels are given in Table 2.2, have been obtained after some initial experiments and from literature [16, 83, 84]. Various sets of experiments have been carried out with the combinations of parameters which are obtained from regression analysis, using Minitab software (V19) as given in Table 2.2. A straight groove of 60 mm was made by linear forward and backward motion of tool, and allowing downward tool travel providing vertical increment at start of each pass. The sample with circular grid and its dimensions is shown in Figure 2.7(b) and 2.7 (c). The samples after the straight groove test are shown in Figure 2.7(d). After the groove is made, the circular marks on the sheet becomes elliptical, and the lengths of the major and minor axes are measured for plane strain analysis. The dome height gives an idea of formability and difference between theoretical depth calculated by step depth times number of cycles run and actual depth accounts for spring back. The output variables have been taken to be major axis length (D_1), minor axis

length (D_2), Number of cycles run till the onset of fracture (N), depth of groove (H), and fabrication time (t). The interaction plots of various output parameters with input variables are shown in Figure 2.8(a)-(d).

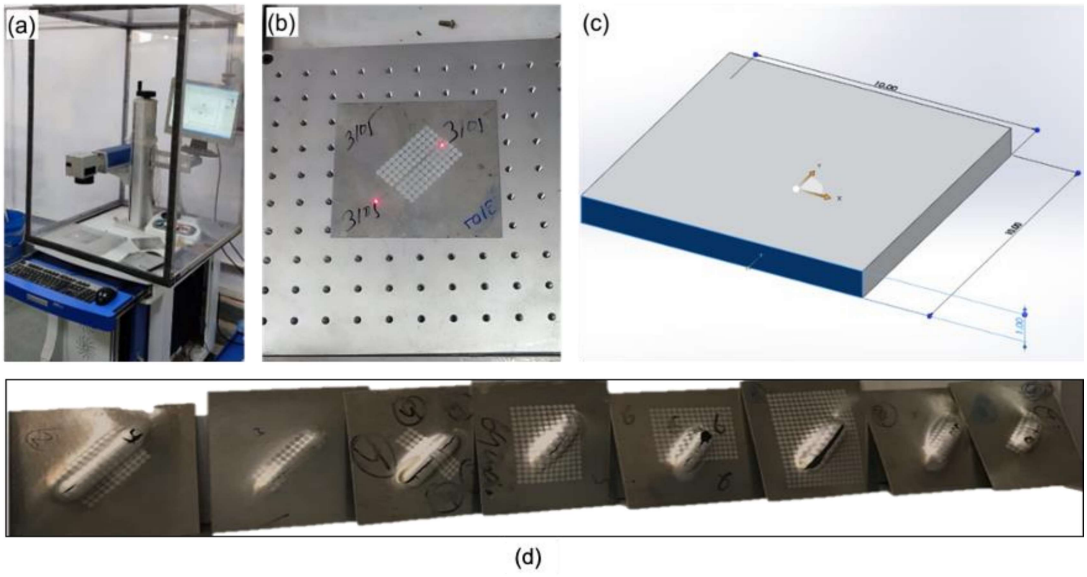

Figure 2.7: Various samples following straight groove test.

Table 2.2: Input parameters in straight groove test

Input Parameters	L (-1)	L (0)	L (1)
Tool diameter (mm)	10	12.5	15
Tool speed (mm/s)	50	100	150
Step depth (mm)	0.2	0.4	0.6

The results of various experiments are presented in Table 2.3. Once all the sets of the experiments are done, the regression model considered the most significant terms and eliminated the insignificant terms or combinations that affected the output response. The dependence of various output parameters on input parameters obtained by Taguchi regression analysis is plotted in Fig. 2.8(a)-(d).

Table 2.3: Results of straight grooves at various input parameters

Exp. No.	Tool Diameter (mm)	Speed (mm/s)	Step depth (mm)	No. of cycles to fracture	Theoretical Depth (mm)	Actual depth (mm)	Major Axis (mm)	Minor axis (mm)	%age spring back	Forming time (s)
1	10.0	50	0.2	87	17.4	15.78	09.36	6.22	09.30	52.2
2	10.0	100	0.4	52	20.8	18.60	09.37	6.10	10.58	15.6
3	10.0	150	0.6	35	21.0	19.25	08.50	5.22	08.33	07.0
4	12.5	50	0.4	48	19.2	17.22	11.23	5.27	10.30	28.8
5	12.5	100	0.6	34	20.4	17.96	10.93	5.13	11.96	10.2
6	12.5	150	0.2	92	18.4	16.82	10.59	5.92	07.74	18.4
7	15.0	50	0.6	29	17.4	16.08	09.27	5.23	07.58	17.4
8	15.0	100	0.2	73	15.6	14.52	08.60	5.34	06.32	21.9
9	15.0	150	0.4	42	16.8	15.60	08.64	5.31	07.14	08.4

The theoretical depth obtained for groove made was calculated by expression (1):

$$Theoretical\ depth = No.of\ cycles\ to\ fracture * Step\ depth \quad (1)$$

However, after release of forming tool the depth of grove made is decreased due to spring back which has been approximated by expression (2).

$$Spring\ back = Theroretical\ depth - Actual\ depth \quad (2)$$

It can be seen from Figure 2.8 (a) that, minimal spring back is observed for tool diameter of 17.5 mm at a forming speed of 100 mm/s and at a step-depth of 0.2 mm. Interaction plot for in-plane major strain has been presented in Figure 2.8 (b). It can be seen maximum in-plane major strain was observed at a forming speed of 50 mm/s with a forming tool of

diameter 15 mm with step depth of 0.4 mm. The forming time was minimum with tool of diameter 10mm and step depth 0.6 mm. The actual forming depth was found to be maximum at a forming speed of 150 mm/s with forming tool of 10 mm diameter and step depth of 0.6 mm.

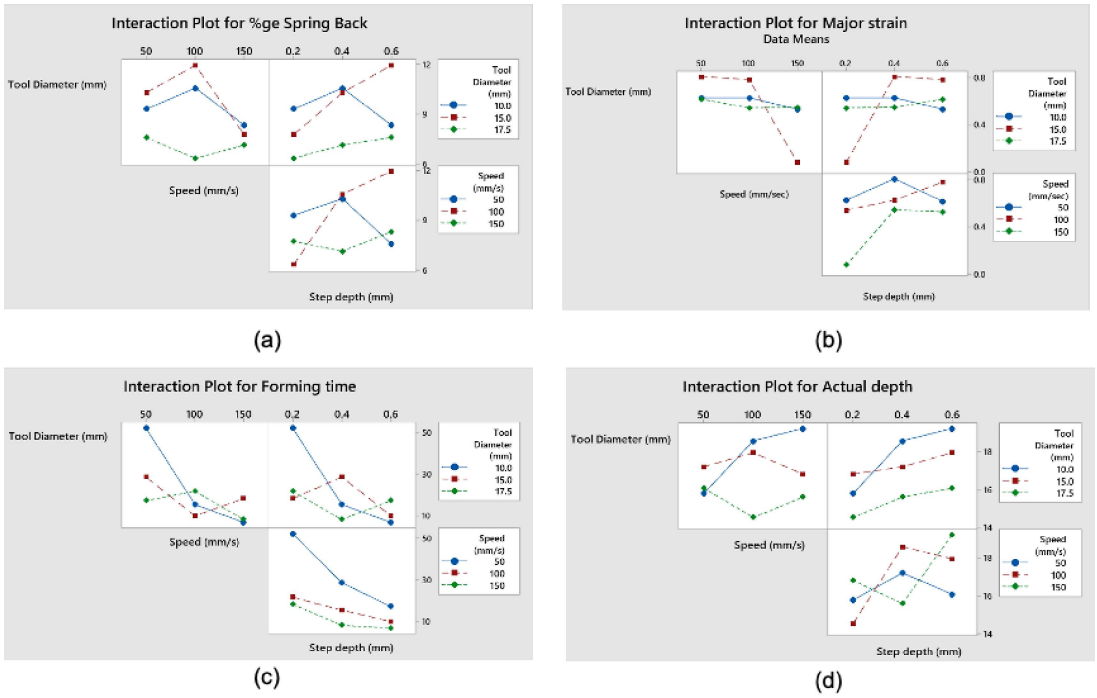

Figure 2.8: (a) Interaction plot of percent spring back on various input parameters, (b) Interaction plot of major strain on various input parameters, (c) Interaction plot of forming time on various input parameters, and (d) Interaction plot of forming depths on various input parameters.

After the regression analysis, the optimum conditions for incremental sheet forming are found to be tool diameter of 10 mm at forming speed of 74.75 m/sec and with a vertical step depth of 0.42 mm which has been taken for all the further experiments and are given in Table 2.4.

Table 2.4: Experimental parameters used for generating 3D shapes.

Parameters used	Optimized value
Type of tool used	Fixed ball tool
Tool Diameter	10 mm
Tool speed	74.75 mm/sec
Step depth	0.42 mm

2.5 Properties of sample before experimentation

The material used for experimentation in this work was aluminium alloy 6061, as aluminium is most widely used in automobile and aerospace industries. Sheets of AA6061 have been taken for experimentation whose thickness was 1.05 mm. Sheets have been fully annealed before forming. For annealing the sheet have been solution heat-treated for 2 hours at 415^0C, cooled in furnace till 260^0C and held for one hour, and finally cooled in air [135]. The composition of the alloy 6061 has been determined by optical emission spectrometer and presented in the Tables 2.5.

Table 2.5: Composition of AA6061

Elements	Al	Ti	Si	Mg	Fe	Mn	Zn	Cr	Cu
Composition (wt %)	97.350	0.050	0.510	0.950	0.410	0.020	0.060	0.151	0.490

2.5.1 Mechanical tests of undeformed sample

2.5.2 Tensile test

In order to assess the material properties of the sheet before forming, uniaxial tensile test and Erichsen cup tests have been conducted. ASTM/E8 standard has been followed in preparation of samples for the tensile test. The tensile plot of undeformed AA6061 is shown in Figure 2.9. The true stress obtained from tensile test has been plotted till UTS only.

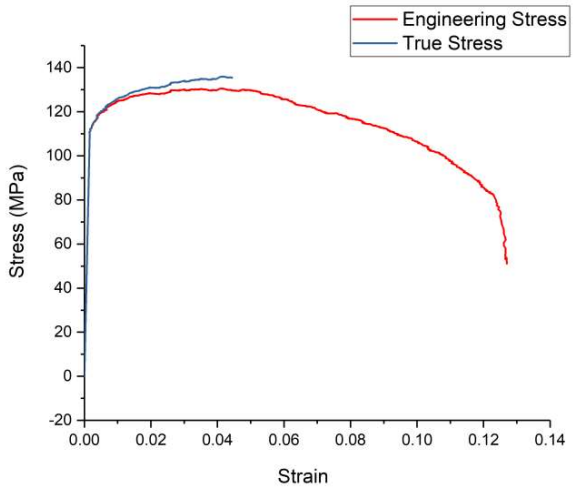

Figure 2.9: Tensile plots of undeformed sample of Al6061.

The mechanical properties obtained from tensile tests are given in Table 2.6.

Table 2.6: Tensile Properties of the alloys 6061, before deformation

Properties	6061
0.2% offset yield strength (MPa)	112
UTS (MPa)	127
Elongation	12.16 %

2.5.3 Erichsen ductility test

In order to predict the formability of ductility test for formability has been performed by the Erichsen cup test, using the set up at the IITBHU. The indenter diameter was 20 mm, main scale division was 1 mm, and the circular scale division was 50/5MSD. Three domes have been formed by indenter till onset of fracture and the depth of the indentation has been measured as (H_E). Domes made on the sheet after Erichsen cup test are shown in Figure 2.10.

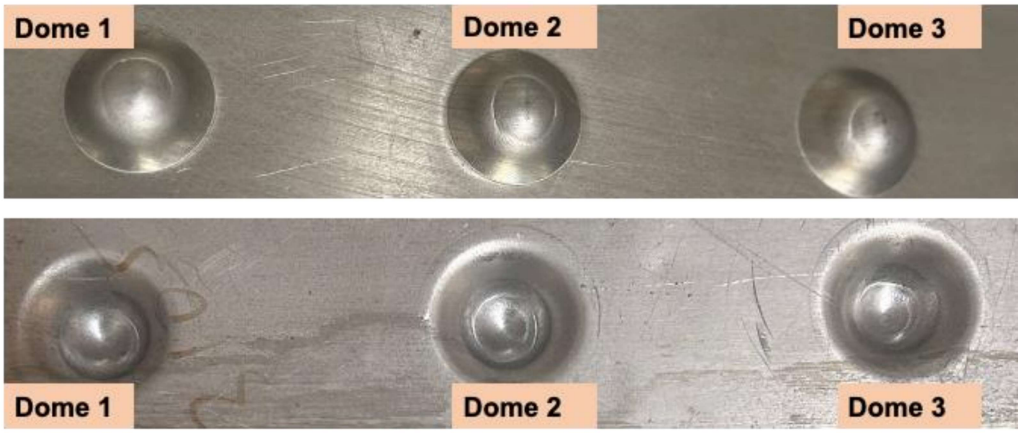

Figure 2.10: Domes formed as a result of indentations during Erichsen cup test

The depth of indentation (H_E) of all the domes on the samples is presented in Table 2.7.

Table 2.7: Result of Erichsen test of the alloys 6061

Parameters	Alloy 6061		
	Dome 1	Dome 2	Dome 3
H_E	9.34	9.12	8.92
Average value of H_E		9.13	

2.6 Formed shapes

Several shapes were made using the strategy explained in Figure 2.5 and 2.6. The experimental parameters for fabricating the AA6061 sheet into these shapes ere the same as optimized by straight groove test and mentioned in Table 2.5. Some of these shapes are given in Figure 2.11.

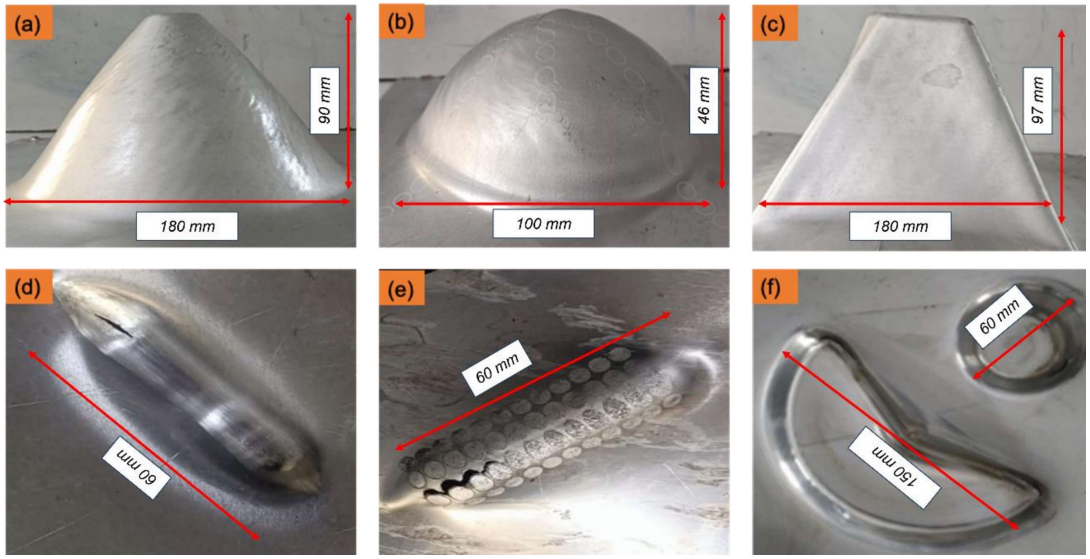

Figure 2.11: Different shapes made by RAISHF (a) Cone with fixed wall angle, (b) hemispherical dome, (c) Rhomboidal frustum, (d) Groove made in straight groove test, (e) Straight groove, and (f) multi-feature shape

It can be seen from Figure 2.11, that ISF is a highly flexible process in which several shapes can be formed without use of dies. Hence the process can be very much cost effective and can play a vital role in the field of small batch production and also for customized production. The process is promising and can be used for industrial application. However, proper understanding of different forces appearing during the process is a must to understand the mechanism behind the process. Additionally, predicting forming forces can also enable the researcher to the process in a much better way. The next chapter deals with development of a mathematical and numerical model for RAISF.